THE JOURNAL OF BIOLOGICAL CHEMISTRY VOL. 286, NO. 44, pp. 38202–38210, November 4, 2011

Novel ATP-driven Pathway of Glycolipid Export Involving TolC Protein*[S]

Received for publication, June 19, 2011, and in revised form, September 13, 2011 Published, JBC Papers in Press, September 14, 2011, DOI 10.1074/jbc.M111.269332

Peter Staron, Karl Forchhammer, and Iris Maldener[1]

From the Department of Microbiology/Organismic Interactions, Interfaculty Institute of Microbiology and Infection Medicine Tübingen, University of Tübingen, 72076 Tübingen, Germany

Background: The ABC exporter DevBCA and the outer membrane protein TolC are necessary for maturation of heterocysts in filamentous cyanobacteria.
Results: DevBCA-TolC form an ATP-driven efflux pump and export heterocyst-specific glycolipids.
Conclusion: DevBCA-TolC provide a novel pathway for glycolipid export.
Significance: Mechanistic details of efflux pumps/ABC exporters are important for understanding various bacterial processes such as cell differentiation, acclimatization processes, or drug resistance.

Upon depletion of combined nitrogen, N_2-fixing heterocysts are formed from vegetative cells in the case of the filamentous cyanobacterium *Anabaena* sp. strain PCC 7120. A heterocyst-specific layer composed of glycolipids (heterocyst envelope glycolipids (HGLs)) that functions as an O_2 diffusion barrier is deposited over the heterocyst outer membrane and is surrounded by an outermost heterocyst polysaccharide envelope. Mutations in any gene of the *devBCA* operon or *tolC* result in the absence of the HGL layer, preventing growth on N_2 used as the sole nitrogen source. However, those mutants do not have impaired HGL synthesis. In this study, we show that DevBCA and TolC form an ATP-driven efflux pump required for the export of HGLs across the Gram-negative cell wall. By performing protein-protein interaction studies (*in vivo* formaldehyde cross-linking, surface plasmon resonance, and isothermal titration calorimetry), we determined the kinetics and stoichiometric relations for the transport process. For sufficient glycolipid export, the membrane fusion protein DevB had to be in a hexameric form to connect the inner membrane factor DevC and the outer membrane factor TolC. A mutation that impaired the ability of DevB to form a hexameric arrangement abolished the ability of DevC to recognize its substrate. The physiological relevance of a hexameric DevB is shown in complementation studies. We provide insights into a novel pathway of glycolipid export across the Gram-negative cell wall.

Efflux pumps are widespread among Gram-negative bacteria and mediate the secretion of various proteins and a wide variety of other molecules (1–5). They bridge the periplasm, allowing a one-step transfer of substrates beyond the outer membrane. Typical efflux pumps consist of three components: (i) an inner membrane factor (IMF),[2] (ii) a periplasmic membrane fusion protein (MFP), and (iii) an outer membrane factor (OMF; supplemental Fig. S1). The OMFs are usually structurally conserved trimers belonging to the TolC superfamily. They form a pore through the outer membrane and extend into the periplasm with an α-helical tunnel-like domain (6–8). MFPs vary in sequence, molecular mass, and biochemical attributes but are similar with respect to the overall structure that includes an α-helical domain, a lipoyl domain, and a β-barrel domain (6, 9–14). IMFs belong to the following three superfamilies that differ with respect to topology, oligomerization state, and energy source: resistance-nodulation-division, major facilitator, and ATP-binding cassette (ABC) (15–17).

Although several proteobacterial efflux pumps have been largely investigated, very little is known about cyanobacterial systems. For the filamentous cyanobacterium *Anabaena* strain PCC 7120, only one potential TolC-involving ABC-type exporter has been proposed on the basis of mutational analysis and *in silico* predictions: DevBCA (also referred to as Alr3710/3711/3712) could possibly be a part of an efflux pump together with the only TolC member predicted in the sequence of *Anabaena* sp. PCC 7120 genome (also referred to as HgdD or Alr2887) (18–22). The *devB* gene is predicted to encode a MFP-like protein; *devC*, the substrate-binding domain of an IMF; and *devA*, the nucleotide-binding domain of an IMF. Mutations in any gene of the *devBCA* operon or *tolC* lead to the loss of one of the key characteristics of *Anabaena* sp.: diazotrophic growth.

Upon depletion of the combined nitrogen source, some of the vegetative cells of the *Anabaena* sp. PCC 7120 filament develop into nitrogen-fixing heterocysts (23). These specialized cells provide the photosynthetic active filament with fixed nitrogen and conversely obtain reductants and carbohydrates for N_2 fixation. Heterocysts inactivate and degrade the oxygen-evolving photosystem II, increase O_2 consumption, and develop a specific envelope outside their Gram-negative cell

* This work was supported by the Deutsche Forschungsgemeinschaft (DFG-Ma1359/5-1).
[S] The on-line version of this article (available at http://www.jbc.org) contains supplemental Tables S1 and S2 and Figs. S1–S4.
[1] To whom correspondence should be addressed: Dept. of Microbiology/Organismic Interactions, Auf der Morgenstelle 28, 72076 Tübingen, Germany. Tel.: 49-7071-29-78847; Fax: 49-7071-29-5843; E-mail: iris.maldener@uni-tuebingen.de.

[2] The abbreviations used are: IMF, inner membrane factor; HGL, heterocyst glycolipid; OMF, outer membrane factor; MFP, membrane fusion protein; ABC, ATP-binding cassette; SPR, surface plasmon resonance; ITC, isothermal titration calorimetry; 8H, octahistidine; 6H, hexahistidine tag; RU, resonance units.

wall to decrease the amount of O_2 that enters into the cell (23, 24). The envelope consists of two distinct layers: the outer layer is composed of polysaccharides (heterocyst envelope polysaccharides) and protects a so-called laminated layer below. The laminated layer represents the actual barrier for O_2 diffusion. It is composed of specific glycolipids (heterocyst envelope glycolipids (HGLs)) (23, 25–27). Several genes encoding proteins putatively involved in synthesis of the HGLs (1-(*O*-α-D-glucopyranosyl)-3,25-hexacosanediol and the 3-ketotautomer) have been identified (28–30); however, the transport of HGLs and assembly of the laminated layer remained unclear. Mutations in *devBCA* or *tolC* result in the absence of the HGL layer, but the synthesis of HGLs is not impaired; therefore, it was assumed that TolC-DevBCA form an efflux pump involved in the transport and/or assembly of the HGL layer (19–21). Nevertheless, it remained unclear which substrate is transported by the postulated TolC-DevBCA machinery across the cell wall. Three possibilities were suggested: (i) transport of HGLs or their moieties, (ii) transport of assembly factors like proteins or unknown compounds required for the formation of the laminated layer, or (iii) both.

In this work, we show that TolC-DevBCA form an ATP-driven efflux pump mediating the export of entire HGLs from the location of their synthesis, the cytoplasmic membrane, to beyond the outer membrane. The exporter requires a distinct stoichiometry that includes a hexameric MFP DevB to recognize and export its substrate.

EXPERIMENTAL PROCEDURES

Anabaena Strains and Growth Conditions—The *Anabaena* strains used in this study are listed in Table 1. Wild-type *Anabaena* sp. PCC 7120 was grown photoautotrophically at 28 °C in liquid $BG11_0$ medium (31). Mutants that could not fix N_2 were grown in $BG11_0$ medium supplemented with 5 mM NH_4Cl and 5 mM TES-NaOH buffer, pH 7.8. The different *Anabaena* mutant strains were grown in the presence of the appropriate antibiotics listed in Table 1 (for applied concentrations, see (18–21)). Media were solidified with 1.5% agar (Difco, Heidelberg, Germany). Induction of heterocyst formation, isolation, and fractioning of cell compartments were performed as described previously (20).

Generation of Mutant Anabaena Strains—All of the *Anabaena* mutants were generated by triparental mating as described previously (32), aiming for single recombination. The mutants $DR181^{TolC\_c6H}$ and $M7^{DevA\_c6H}$ (pIM318/322 constructs listed in supplemental Table S1) were generated by the conjugation of pRL271 ligated to XhoI fragments containing amplified *tolC* or *devA* fused to a 3′-hexahistidine tag (supplemental Table S2: oligonucleotides 271_TolC_c6H/271_DevA_c6H). To generate the templates for those fusion inserts, both genes were cloned into pQE60 (Qiagen, Hilden, Germany) by ligating total DNA amplified products via NcoI and BamHI (oligonucleotides 60_TolC_c6H/60_DevA_c6H).

The mutants $DR74^{DevB}$ (pIM442 construct, supplemental Table S1) and $DR74^{DevB\_N333A}$ (pIM444) were complemented by the conjugation of pCSEL24 (33) ligated to EcoRI and PstI fragments containing total DNA-amplified *devBCA* or $devB^{N333A}CA$ (supplemental Table S2: oligonucleotides 24_BCA). The $devB^{N333A}CA$ mutation was introduced by using primers directly flanking and overlapping the region to be mutated (oligonucleotides DevB_N333A).

Expression Analysis—Total RNA was extracted from 50-ml samples of *Anabaena* cultures in different states of combined nitrogen deprivation (before and at 3, 6, 9, 12, and 24 h after nitrogen step-down; as described in Ref. 20) by using the High Pure RNA Isolation Kit (Roche Applied Science, Mannheim, Germany), according to the manufacturer's instructions. RNA samples were reverse transcribed and amplified using the One Step RT-PCR Kit (Qiagen), according to the manufacturer's instructions. For *rnpB* amplification, the RNA samples were boiled at 95 °C for 5 min before amplification. The primers used for RT-PCR are listed in supplemental Table S2. The products were analyzed on a 2% agarose gel stained with 0.05% ethidium bromide.

Construction, Overexpression, and Purification of Recombinant Proteins—TolC, DevB, and DevAC were overexpressed as GST-tagged fusion proteins in *Escherichia coli* strain Rosetta-Gami™(DE3) (Merck, Darmstadt, Germany) by using the multitag expression vector pET42a (Merck; supplemental Table S2, oligonucleotides 42_TolC, 42_DevB, and 42_DevAC). Recombinant proteins were purified using GST SpinTrap or GSTrap FF columns (GE Healthcare). The N-terminal GST tag was cleaved off using Factor Xa, and the protease was removed using Xa Removal Resin (Qiagen). According to the role of the respective construct in interaction studies, the protein designed to be immobilized carried a C-terminal octahistidine tag (8H; from pET42a) if a tag had not already been introduced inside the protein (Table 2).

To ensure that a high amount of soluble protein was available for *in vitro* experiments, a membrane barrel-free version of TolC was constructed. OM-barrel-forming amino acids located between positions 365 and 417 and between positions 587 and 624 were replaced with four repeats of G and S (4GS; pIM378 construct, supplemental Table S1) or an octahistidine tag (pIM380). Both constructs were amplified as PCR fusion products by using primers directly flanking the predicted barrel elements and carrying respective self-priming sequences as a 3′ clamp (oligonucleotides TolC_iGS and TolC_i8H). The first 287 N-terminal amino acids of the predicted TolC protein were not taken into account for the constructs used in this work. BLAST analysis showed that they were not clearly related to any known function and are not present in other known TolC systems. The full-length TolC was highly unstable *in vitro* (data not shown).

All of the *in vitro* DevB constructs were amplified after replacing the membrane anchor region (amino acids 23–40) with GS repeats (oligonucleotides DevB_MA). The α-hairpin 8H tag DevB variant (pIM384) was constructed by fusing PCR products as described for the TolC constructs above (oligonucleotides DevB_i8H). The mutation V469C (pIM397; oligonucleotides DevB_V469C) was introduced as described for mutant $DR74^{DevB\_N333A}$. The amino acids to be replaced and/or omitted in TolC and DevB were predicted using models and methods as described previously (20).

DevC and DevA were fused by omitting the stop codon of *devA* and placing *devA* in the 5′ region of *devC*, linked via a 4GS

TABLE 1

***Anabaena* strains used in this work**

alr2887 = *tolC* (referred as *hgdD* in Ref. 20), *alr3710* = *devB*, *alr3711* = *devC*, *alr3712* = *devA*. $Fox^{+/-}$, is able/is not able to fix N_2 under aerobic conditions; Hgl^+, produces HGLs.

Anabaena strain	Genotype	Resistance	Properties	Source
PCC 7120	Wild-type		Fox^+Hgl^+	C. P. Wolk
DR181	*alr2887*::*C.K3*	Nm^r	Fox^-Hgl^+	Ref. 20
$DR181^{TolC\_c6H}$	*alr2887*::*C.K3*, *alr2887′*::$alr2887^{c6H,a}$	Nm^r, Cm^r, Em^r	Fox^+Hgl^+	This work
M7	*alr3712*::*Tn5*	Nm^r, Sm^r,	Fox^-Hgl^+	Ref. 18
$M7^{DevA\_c6H}$	*alr3712*::*Tn5* + *alr3712′*::$alr3712^{c6H,a}$	Nm^r, Sm^r, Cm^r, Em^r	Fox^+Hgl^+	This work
DR74	*alr3710*::*C.K3*	Nm^r	Fox^-Hgl^+	Ref. 18
$DR74^{DevB}$	*alr3710*::*C.K3* + *nucA*::$alr3710\text{-}12^b$	Nm^r, Sm^r, Sp^r	Fox^+Hgl^+	This work
$DR74^{DevB\_N333A}$	*alr3710*::*C.K3* + *nucA*::$alr3710^{N333A}\text{-}12^b$	Nm^r, Sm^r, Sp^r	Fox^-Hgl^+	This work

[a] Single recombination of pRL271, including *tolC* or *devA* into the 5′ region of the respective gene.
[b] Recombination of pCSEL24, including *devBCA* or $devB^{N333A}CA$ into *nucA* of the α-plasmid of *Anabaena* sp. PCC 7120.

or 8H sequence (pIM409/410 constructs; oligonucleotides 42_DevAC, DevAC_iGS, and DevAC_i8H).

In Vivo Cross-linking—*Anabaena* strains $DR181^{TolC\_c6H}$ or $M7^{DevA\_c6H}$ (Table 1) were deprived of combined nitrogen for 9 h in 50 ml of $BG11_0$ medium. To obtain a final concentration of 0.5% formaldehyde in the culture, 7.15 ml of a prewarmed (overnight at 70 °C) paraformaldehyde solution (4% in PBS, pH 7.4, 10 mM Na_2HPO_4, 1.8 mM KH_2PO_4, 137 mM NaCl, and 2.7 mM KCl) was added. The cross-linking reaction was quenched after 5–20 min by washing the culture three times with 100 mM Tris-NaOH buffer, pH 8.0. The cells were broken by 10 passes through a French pressure cell (24,000 psi) and separated into a soluble cytoplasmic/periplasmic and an insoluble membrane fraction by centrifugation (30,000 × *g*, 30 min, 4 °C). The debris was solubilized with a final concentration of 0.1% Triton X-100 for 30 min at 25 °C. After consecutive centrifugation (30,000 × *g*, 30 min, 4 °C), the supernatant was purified with nickel-nitrilotriacetic acid spin columns (Qiagen), according to the manufacturer's instructions. To remove cross-linking methylene bridges, the eluate was incubated for 30 min at 75 °C in a modified SDS sample buffer (final concentration, 10 mM Tris, pH 6.8; 0.5% SDS; 2% glycerol; and 150 mM mercaptoethanol). The proteins were separated on a 10% SDS-PAGE with subsequent colloidal Coomassie G staining (34) or transferred to a PVDF membrane for immunodetection.

Immunodetection—PVDF membranes were blocked for 10 min with TBS buffer (20 mM Tris-HCl, pH 7.5, 150 mM NaCl) containing 1% powdered milk and then incubated with primary antibody solution (in TBS containing 0.1% powdered milk) at 4 °C overnight. After three consecutive washes with TBS, the membrane was incubated with horseradish peroxidase-conjugated secondary α-rabbit antibody (1:100,000; Sigma-Aldrich, Munich, Germany) for 1 h at room temperature. The signals were captured using a Kodak Gel Logic 1500 imaging system. The primary antibodies used for Western blotting were αTolC (αD; 1:10,000), αDevB (αB; 1:2500), αDevC (αC; 1:10,000), and αDevA (αA; 1:25,000). The antibodies αDevC, αDevA, and αTolC were raised against the purified His-tagged full-length proteins by Pineda, Munich, Germany (data not shown). DevB antibodies were raised against the peptide sequences NRIRAEQRNAQVDAG and AISQQERDRRRLTATT by Pineda.

Surface Plasmon Resonance—Surface plasmon resonance (SPR) experiments were performed using a Biacore X biosensor system (Biacore AB, Uppsala, Sweden) as described previously (35). Purified recombinant His-tagged proteins were bound to flow cell 2 (FC2) of a Ni^{2+}-loaded nitrilotriacetic acid sensor chip prepared according to instructions from Biacore. Thiol coupling was performed as reported previously (10). Binding assays were performed in reaction buffer (25 mM MES-NaOH at pH 6.0–6.4 or HEPES-NaOH at pH 7.0, 150 mM NaCl, and 0.05% Triton X-100) at 25 °C. Samples were injected into the FC1 and FC2 of the sensor chip at a flow rate of 20 μl/min, and the response difference (FC2-FC1) was recorded. The reaction parameters were calculated from received data and fitted using the BiaEvaluation (Biacore AB) and Origin (version 6.0, OriginLab, Northampton) software.

Isothermal Titration Calorimetry—Isothermal titration calorimetry (ITC) experiments were performed in reaction buffer (25 mM MES-NaOH buffer, pH 6.2, 150 mM NaCl, and 0.05% Triton X-100) at 25 °C, using a VP-ITC microcalorimeter (MicroCal, GE Healthcare). In experiments with TolC and DevB, a 10 μM TolC solution ($TolC^{sol}$_iGS construct, Table 2) was titrated with 100 μM of DevB ($DevB^{sol}$). In experiments with DevAC and DevB, a 3 μM DevAC (DevAC_iGS, Table 2) solution was titrated with 30 μM of DevB ($DevB^{sol}$). Ten microliters of the ligand solution were injected each of 40 times into the 1.43-ml cell, with stirring at 350 rpm. The interaction parameters were calculated using MicroCal Origin software.

Chromatography—DevB oligomerization was analyzed via a gel filtration column (HiLoad 26/60-Superdex, GE Healthcare). The column was equilibrated with reaction buffer (25 mM MES-NaOH, pH 6.2, 150 mM NaCl, and 0.05% Triton X-100), and the proteins (0.1 mg/ml) were injected in the same reaction buffer, at a flow rate of 1 ml/min. The molecular mass standards used were β-amylase (200 kDa), β-galactosidase (116 kDa), BSA (66 kDa), and carbonic anhydrase (29 kDa).

Lipid Analysis—Total lipids were extracted from filaments, isolated heterocysts, or cell fractions by adding a methanol-chloroform mixture (1:2). The organic solvent was evaporated in a stream of air. The lipids were dissolved in 200 μl of chloroform and chromatographed on thin-layer plates of silica gel (Kieselgel 60, Merck) in 170 ml of chloroform, 30 ml of methanol, 20 ml of acetic acid, and 7.4 ml of distilled water. Lipids were visualized by sprinkling the plate with 25% sulfuric acid and exposing it to 200 °C for 90–120 s. Pure HGLs were prepared as described in Ref. 36, and cell fractions were prepared as described in Ref. 20.

ATP Hydrolysis Assay—The assay was performed with 0.1 μg/ml DevAC and 0.2 μg/ml DevB and indicated concentrations of substrate mixes in ATPase reaction buffer (50 mM

TABLE 2
Protein derivatives used in this work
Primers used for construction are listed in supplemental Table S2.

Construct	Modification	Purpose
TolC^{sol}_iGS	Membrane barrel replaced (2 × 4GS instead)	SPR, ITC
TolC^{sol}_i8H	Membrane barrel replaced (2 × 8H instead)	SPR
TolC_c6H	C-terminal 6H	Cross-link bait
DevB^{sol}	Membrane anchor replaced (GS instead)	SPR, ITC
DevB^{sol}_c8H	Membrane anchor replaced (GS instead), C-terminal 8H	SPR
DevB^{sol}_i8H	Membrane anchor replaced (GS instead), hairpin 8H	SPR
DevB^{sol}_V469C	Membrane anchor replaced (GS instead), V469C	SPR
DevB^{sol}_N333A	Membrane anchor replaced (GS instead), N333A	SPR
DevB_N333A	N333A	Complementation
DevAC_iGS	Stop codon of DevA removed, 4GS between DevA and DevC	SPR, ITC
DevAC_i8H	Stop codon of DevA removed, 8H between DevA and DevC	SPR
DevA_c6H	C-terminal 6H	Cross-link bait

MES-NaOH, pH 6.5, 1.5 mM DTT, and 0.05% Triton X-100) supplemented with a regeneration system (6 mM P-enolpyruvate, 3 μg/ml pyruvate kinase), 3 μg/ml lactate dehydrogenase, 0.5 mM NADH, and 2 mM ATP at 25 °C. Absorbance data were collected at 340 nm using a SPECORD 205 spectrophotometer (Analytik Jena AG) and evaluated using the WinASPECT software (version 2.2.1.0). The rate of hydrolysis in units was calculated as mol of ATP hydrolyzed per minute and per milligram of the ATPase DevAC.

Electron Microscopy—Samples for transmission electron microscopy were prepared as described previously (19). In brief, fixation and post-fixation were performed using glutaraldehyde and potassium permanganate; ultrathin sections were stained with uranyl acetate and lead citrate. The samples were examined with a Philips Tecnai electron microscope at 80 kV.

RESULTS

TolC Interacts with DevBCA in Vivo—Because of the similar phenotypes of mutants in *devBCA* and *tolC* and sequence similarities to proteobacterial secretion systems, previous studies proposed that TolC (also referred to as Alr2887 and HgdD) of *Anabaena* sp. PCC 7120 forms a secretion complex with DevBCA (20, 21). Cross-linking experiments were performed to clarify whether the subunits of this putative efflux pump interact *in vivo*. According to a typical model of this type of exporter, TolC in the outer membrane and DevA in the cytoplasm/cytoplasmic membrane should be the most distant participants (supplemental Fig. S1). Therefore, these proteins were fused to a His tag and used as baits for the rest of DevBCA-TolC. To obtain the best yield rate, the maximum protein expression of the proteins during heterocyst induction by nitrogen stepdown was investigated. In our immunoblots and RT-PCR analysis, we confirmed previous transcription studies of *tolC* and *devB* (19–21). TolC and DevB showed maximum expression at 9 h after depletion of combined nitrogen (Fig. 1*A*). The filaments that had been depleted of combined nitrogen for 9 h were chosen for cross-linking experiments.

Using cells expressing His-tagged TolC (TolC_c6H in Table 2), a dominant TolC band (Fig. 1*B*, *SDS*+ at ~75 kDa and *αD*) and several weaker bands of lower mass (Fig. 1*B*, *SDS*+) were obtained after formaldehyde cross-linking and purification of the bait. Some of the lower bands could be identified using specific antibodies against DevB, DevC, and DevA in immunoblots. DevB and DevC were easily detectable (Fig. 1*B*, dominant bands in *lanes αB* and *αC*, respectively). A weak band corresponding to the molecular weight of DevA was obtained in longer exposed immunoblots (Fig. 1*B*, *αA*). Other proteins could not be detected in an eluate from non-cross-linked cell extracts (Fig. 1*B*, *SDS*−).

A similar cross-linking approach was used with cells expressing His-tagged DevA as bait (DevA_c6H in Table 2 and Fig. 1*C*). DevA_c6H was the only detectable band in eluants from non-cross-linked cell extracts (Fig. 1*C*, *SDS*− at ~28 kDa), whereas it eluted together with a couple of bands of higher mass in the presence of 0.5% formaldehyde (Fig. 1*C*, *SDS*+). All of the four assumed participants of the DevBCA-TolC complex could be detected readily by immunoblotting (Fig. 1*C*, *αA*, *αC*, *αB*, and *αD*). In contrast to using TolC_c6H as bait, less cross-reacting bands could be detected with antibodies against DevB and DevC (Fig. 1*C*; *αB* and *αC*).

In summary, the four components seem to be at least in very close proximity. The proposed *in vivo* interaction of DevBCA and TolC (20) seems likely.

DevB Hexamer Completes TolC-DevBCA Efflux Pump—To confirm the *in vivo* results, we investigated the interaction between distinct partners of the proposed complex by using SPR. First, the binding of DevB (DevB^{sol} construct in Table 2) to the chip surface-bound TolC (TolC^{sol}_i8H) was analyzed. Roughly in agreement with the results obtained for the homologue systems from *E. coli* (10), the highest response occurred at an acidic pH of 6.2, whereas interaction was remarkably impaired at higher pH values (Fig. 2*A*). To exclude an unwanted effect of the His tag due to the low pH used, thiol coupling of DevB onto the chip surface was used instead of His-tagged protein to verify the reaction optimum. The pH optimum obtained using this approach was the same as that obtained using His-tagged proteins (supplemental Fig. S2).

The best fit for TolC-DevB interaction at pH 6.2 was obtained by evaluating the SPR data in a two-stage binding model (heterogeneous ligand model in BiaEvaluation software). The affinities of surface-bound TolC (TolC^{sol}_i8H in Table 2) to DevB (DevB^{sol}) were K_{d1} = 37 nM and K_{d2} = 110 nM (Fig. 2*B*). Although higher surface densities of TolC did not affect the binding constants and/or fitting model, they were crucial in the case of surface-bound DevB (DevB^{sol}_c8H). Compared with the interaction of immobilized TolC (~440 RU) to ligand DevB (Fig. 2*B*), more mass of immobilized DevB (~2400 RU) was necessary to

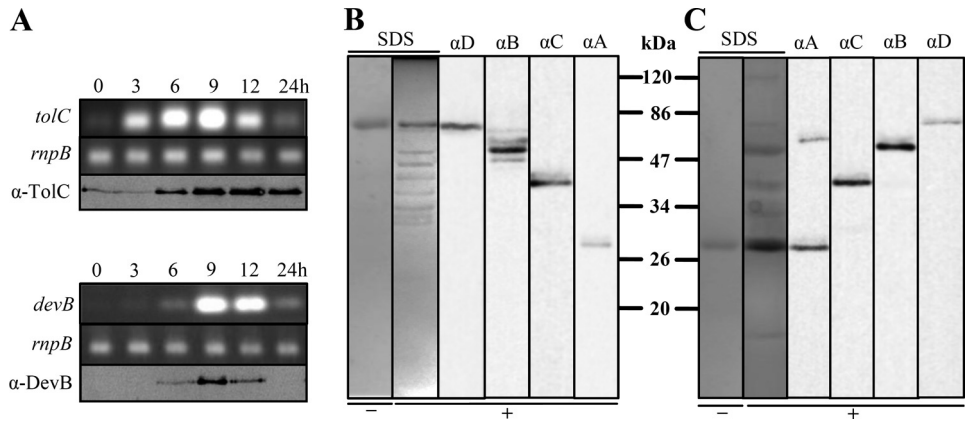

FIGURE 1. **Expression pattern of *devB* and *tolC* and interaction of TolC-DevBCA *in vivo*.** *A*, time-dependent expression pattern of *tolC* and *devB* analyzed by RT-PCR (*italic*) or immunoblots. *RnpB* refers to the loading control ribonuclease B. RNA or cell extracts were obtained from the same culture after indicated time points of nitrogen starvation. *B*, formaldehyde cross-link of His-tagged TolC *in vivo*. After 9 h of nitrogen starvation, filaments of mutant DR181^{TolC_c6H} were treated with 0.5% formaldehyde for 15 min (+). His-tagged TolC (TolC_c6H; Table 2) was purified and separated via SDS-PAGE. The proteins were stained with colloidal Coomassie G (SDS) or transferred to a PVDF membrane for immunodetection of TolC (*αD*), DevB (*αB*), DevC (*αC*), or DevA (*αA*). A purified sample of TolC-c6H from DR181^{TolC_c6H} without addition of formaldehyde was loaded on a SDS gel for control (−). *C*, formaldehyde cross-link of His-tagged DevA *in vivo*. DevA_c6H and the mutant M7^{DevA_c6H} were treated as described for TolC_c6H and mutant DR181^{TolC_c6H} in *B*.

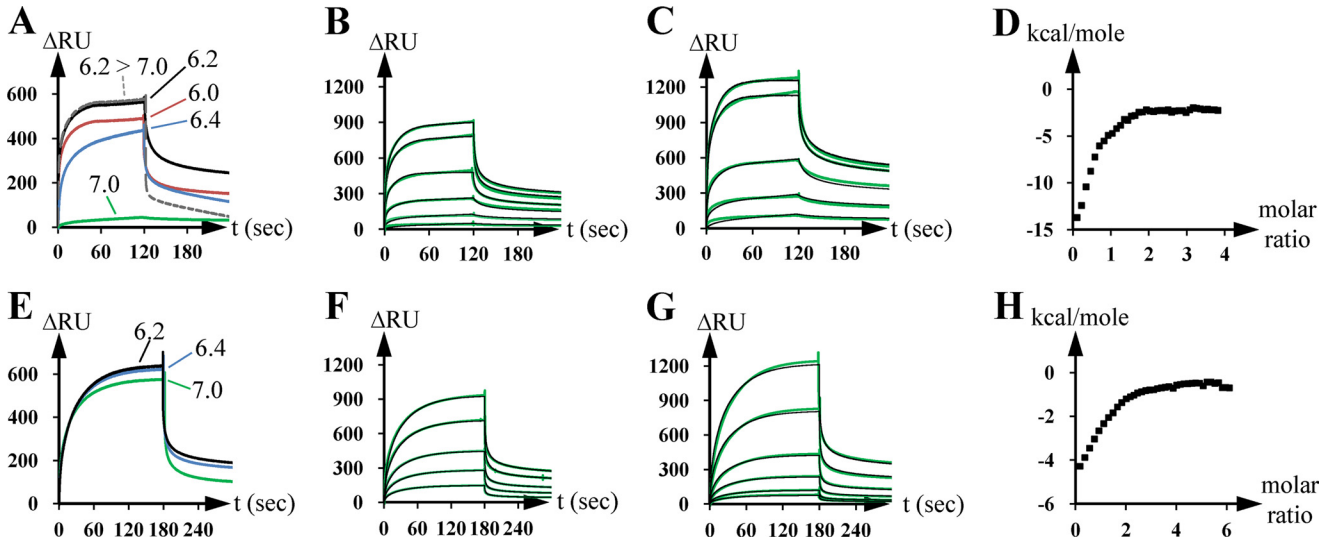

FIGURE 2. **Interaction of the OMF TolC with the MFP DevB and of the IMF DevAC with DevB *in vitro*.** *A*, SPR analysis of the interaction of immobilized TolC (TolC^{sol}_i8H in Table 2; ~400 RU) with DevB (DevB^{sol}; 0.8 μM) in dependence of indicated pH values. *B*, SPR analysis of the interaction of immobilized TolC (TolC^{sol}_i8H; ~440 RU) to DevB (DevB^{sol}). DevB was injected at concentrations doubling from 0.05 μM to 1.6 μM. The *green lines* show the experimental data, the *black lines* the fit by using a two-stage/heterogeneous ligand model. *C*, SPR analysis of the interaction of immobilized DevB (DevB^{sol}_c8H; ~2400 RU) to TolC (TolC^{sol}_iGS). TolC was injected at concentrations doubling from 0.1 to 1.6 μM. The *green lines* show the experimental data, and the *black lines* show the fit by using a two-stage/heterogeneous ligand model. *D*, ITC analysis of the interaction of TolC (TolC^{sol}_iGS) to DevB (DevB^{sol}). 10 μM TolC were titrated 40 times with 100 μM DevB at pH 6.2. The *squares* represent the measured and integrated energy release peaks. *E*, SPR analysis of the interaction of immobilized DevAC (DevAC_i8H; ~440 RU) to DevB (DevB^{sol}; 0.8 μM) in dependence of indicated pH values. *F*, SPR analysis of the interaction of immobilized DevAC (DevAC_i8H; ~470 RU) to DevB (DevB^{sol}). DevB was injected at concentrations doubling from 0.05 to 1.6 μM. The *green lines* show the experimental data, and the *black lines* show the fit by using a two-stage/heterogeneous ligand model. *G*, SPR analysis of the interaction of surface-bound DevB (DevB^{sol}_i8H; ~2400 RU) to DevAC (DevAC_iGS). DevAC was injected at concentrations doubling from 0.1 to 1.6 μM. The *green lines* show the experimental data, and the *black lines* show the fit by using a two-stage/heterogeneous ligand model. *H*, ITC analysis of the interaction of DevAC (DevAC_iGS) to DevB (DevB^{sol}). 3 μM DevAC were titrated 40 times with 30 μM DevB at pH 6.2. The *squares* represent the measured and integrated energy release peaks.

obtain similar binding constants to ligand TolC (TolC^{sol}_iGS, Fig. 2*C*). Binding constants of immobilized DevB to ligand TolC were K_{d1} = 55 nM and K_{d2} = 140 nM (Fig. 2*C*). Applying lower surface densities of DevB led to a different and highly complex evaluation. To clarify this issue, we repeated the interaction experiment using a surface- and orientation-independent ITC approach (Fig. 2*D*). Consistent with the results of the SPR experiments, the ITC data provided the best fit on using a two-stage model. The binding constants of TolC (TolC^{sol}_iGS) to injected DevB (DevB^{sol}) were K_{d1} = 88 nM and K_{d2} = 380 nM.

Interestingly, both approaches predicted saturation of DevB binding to TolC near to a molar ratio of 2:1 (ITC in Fig. 2*D*; SPR in Fig. 2, *B* and *C*). A saturation molar ratio of ~1.72:1 for the binding of DevB to TolC was obtained from ITC data, whereas the ratio found to be ~1.71:1 (~900 RU of 51.9-kDa DevB bound to ~440 RU of immobilized 43.5-kDa TolC, Fig. 2*B*) or ~1.54:1 (~1240 RU of 42.3-kDa TolC bound to ~2400 RU of immobilized 53.1-kDa DevB, Fig. 2*C*) upon using SPR. The use of higher ligand concentrations did not considerably increase the response (data not shown).

Next, the interaction between the MFP DevB and the IMF DevC was investigated. Studies on proteobacterial ABC exporter systems have reported that the nucleotide-binding domain (corresponding to DevA) and the substrate-binding domain (DevC) of the respective IMF can be located together on one polypeptide (15, 37–39). To avoid artifacts caused by missing protein parts, DevAC hybrids (42_DevAC and DevAC_iGS or DevAC_i8H in Table 2) were used instead of DevC alone. Similar to the results obtained for the binding of DevB to TolC (Fig. 2*A*), the pH optimum of the DevB response toward immobilized DevAC was 6.2 (Fig. 2*E*), but the response did not change considerably until pH 7.0.

The best fit for SPR data for the interaction of immobilized DevAC (DevAC_i8H in Table 2) to DevB ($DevB^{sol}$) was also obtained by using a two-stage binding model, resulting in the binding constants K_{d1} = 940 nM and K_{d2} = 3911 nM (Fig. 2*F*). The surface density of immobilized DevAC did not have a remarkable influence on the reaction, but low surface densities of immobilized DevB led to problems similar to those described for the interaction between TolC and immobilized DevB. The binding constants of immobilized DevB ($DevB^{sol}$_i8H) to DevAC (DevAC_i8GS) were K_{d1} = 531 nM and K_{d2} = 3708 nM (Fig. 2*G*).

The response saturation data predicted a DevB to DevAC ratio of nearly 3:1. In the case of immobilized DevAC, it was 2.84:1 (~970 RU of 51.9-kDa DevB bound to ~470 RU of immobilized 71.3-kDa DevAC, Fig. 2*F*), and in the case of surface-bound DevB, it was 2.64:1 (~1220 RU of 71.2-kDa DevAC bound to ~2400 RU of immobilized 53.1-kDa DevB, Fig. 2*G*). ITC data predicted a reaction saturation at a DevB:DevAC ratio of 2.90:1 (Fig. 2*H*).

In summary, the results of our *in vitro* studies show that TolC, DevB, and DevAC interact in a molar ratio of 3:6:2 (on assuming average DevB:TolC and DevB:DevAC ratios of 2:1 and 3:1, respectively). Such molar ratios have been postulated earlier for the ATP-driven efflux pump MacAB-TolC (40–42). Our data indicate that TolC and DevBCA also seem to form an ATP-driven efflux pump (because *devA* is predicted to encode an ATPase), as hypothesized in earlier studies (18–20).

HGLs Are a Substrate for TolC-DevBCA—HGLs, their moieties, or accessory factors necessary for the formation of the laminated layer could be substrates of DevBCA-TolC. Missing any of these components would result in the phenotype of the *devBCA*/*tolC* mutants (19, 20). To identify substrates of DevBCA-TolC, we exposed the IMF and ATPase DevAC and the MFP DevB (Fig. 3*A*, *ACB*) to complex substrate mixes such as whole-cell extracts of *Anabaena*, membranes, and soluble fractions (Fig. 3*B* reflects the lipid composition of the fractions). The ATP-hydrolyzing activity slightly increased in the presence of whole-cell extracts of cells depleted of nitrogen for 9 h (Fig. 3*A*, *HCE*). Heterocyst membranes (cell wall and cytoplasmic and thylakoid membranes) were slightly better enhancers (Fig. 3*A*, *HMF*), whereas heterocyst cell walls caused an even stronger enhancement (Fig. 3*A*, *HCW*). DevACB activity was not modified by pretreating the cell wall fractions with proteinase K, so the substrates should not be proteinaceous (data not shown). The only known differences between the cell walls of heterocysts and vegetative cells are protein (43) and the additional layers (polysaccharide and glycolipids) of the heterocyst. Finally, purified HGLs were used as substrates in the ATPase assay with DevBCA. This exposure caused a nearly 7-fold boost in the rate of ATP hydrolysis (Fig. 3, *A* and *B*, *HGL*).

The TolC knock-out mutant DR181 forms a heterocyst envelope polysaccharide layer and synthesizes HGLs but does not assemble an HGL layer (21). The cell walls of the heterocysts of this mutant did not remarkably affect the ATPase activity of DevACB (Fig. 3*A*, *MCW*). On using the cytoplasmic membrane fraction, where the glycolipids get stuck in DR181 (compare devB mutant in Fig. 3*B*, MT), an increase could be observed in the ATPase activity (Fig. 3*A*, *MCM*).

The response of DevACB was proportional to the amount of fractions containing HGLs (Fig. 3*A* and supplemental Fig. S4, *gray bars*), whereas no enhancement of ATP activity was detected using fractions not containing HGLs (Fig. 3*A* and supplemental Fig. S4, *white bars*). Therefore, the glycolipids are good candidates for DevBCA-TolC substrates. It has to be noted that substrate-dependent activation of the ATPase activity of DevAC toward the presence of HGLs was observed only in the presence of the DevB (Fig. 3*A*, *ACB* and *AC*).

A mutation at Asn-333 to Ala in DevB abolished the ability of $DevACB^{N333A}$ to respond to HGLs (Fig. 3*A*, *MT*). This mutation impaired DevB hexamer formation (supplemental Fig. S3). SPR data from DevB_N333A interaction with surface-bound TolC or DevAC showed altered binding and could not predict the TolC:DevB:DevAC molar ratio of 3:6:2 described above (Fig. 3*C*). This stoichiometry is crucial for *in vivo* function of the HGL exporter: complementation of the *devB* mutant DR74 with a wild-type copy of *devB* results in a functional HGL layer (Fig. 3*D*, $DR74^{DevB}$), whereas the mutant N333A could not rescue the DR74 phenotype. Heterocysts of mutant $DR74^{DevB\_N333A}$ lack the glycolipid layer (Fig. 3*E*), and the HGLs stay in the cytoplasmic membrane (Fig. 3*B*, *HCM/MT*).

The mutated version of the MFP DevB could not fulfill its function in exporting HGLs. The ability to form stable hexamers is a prerequisite for the transport process of HGLs.

DISCUSSION

In recent years, numerous genes of *Anabaena* sp. PCC 7120, which encode enzymes involved in the synthesis of special polysaccharides, heterocyst glycolipids, and components of the heterocyst envelope, have been identified in studies that mostly involved transposon mutagenesis (reviewed in Ref. 43). However, the mechanism by which the molecules traverse the Gram-negative cell wall of the developing heterocyst remained unknown. The data presented in this study show that DevB, DevC, DevA, and TolC form an ATP-driven efflux pump for the export of HGLs. This system is, to our knowledge, the first of its kind described for the synthesis of the unique Gram-negative cell envelope of heterocysts.

Promiscuous Role of TolC—Both *devB*, the first gene of the *devBCA* operon, and *tolC* are induced during heterocyst differentiation, showing maximum abundance at 9 h after nitrogen step-down. The signal strength of TolC remained constant but that of DevB/*devB* decreased rapidly. This could be due to the specific contribution of DevBCA to the developing cell wall of heterocysts (export of HGLs). TolC-like proteins have been

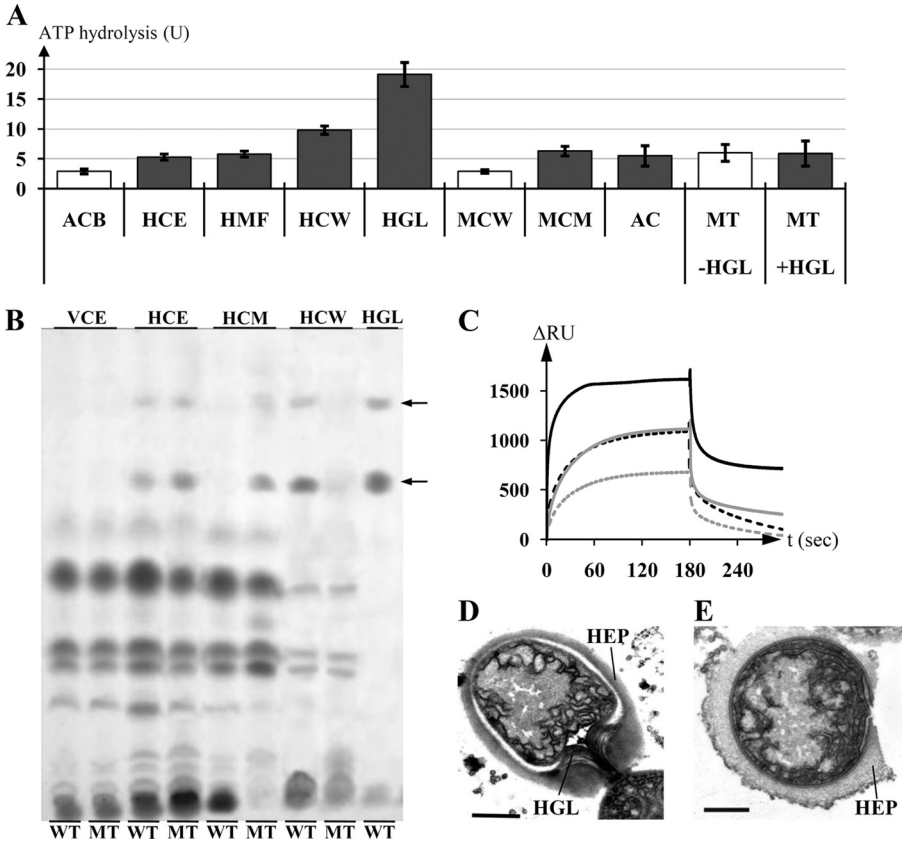

FIGURE 3. **The substrate of TolC-DevBCA.** *A*, ATP hydrolysis rates of DevAC in presence of indicated substrate mixes. *ACB* represents DevAC with DevB; *HCE* represents DevAC, DevB, and heterocyst cell extract; *HMF* represents DevAC, DevB, and heterocyst membranes; *HCW* represents DevAC, DevB, and heterocyst cell walls; *HGL* represents DevAC, DevB, and purified HGLs; *MCW* represents DevAC, DevB, and cell walls of mutant DR181; *MCM* represents DevAC, DevB, and cytoplasmic membranes of mutant DR181; *AC* represents DevAC without DevB; *MT* represents DevAC and $DevB^{N333A}$, *+/−HGL* represents with/without purified HGLs. All substrate concentrations were adjusted to 4 μg of the respective protein fraction or equal to 4 μg cell wall protein in the case of adding HGLs. *Gray bars* indicate the presence of HGLs in the respective fractions. ATPases possibly present inside the substrate fractions were preinactivated by incubation with 5 mM VaO_4. *B*, thin layer chromatography of extracts of complemented mutants $DR74^{DevB}$ and $DR74^{DevB\_N333A}$, and purified HGLs. *WT*, $DR74^{DevB}$; *MT*, $DR74^{DevB\_N333A}$; *VCE*, vegetative cell extract; *HCE*, heterocyst cell extract; *HCM*, heterocyst cytoplasmic membranes; *HCW*, heterocyst cell walls; *HGL*, purified HGLs. *Arrows* indicate HGLs. *C*, SPR analysis of the interaction of either immobilized TolC ($TolC^{sol}$_i8H; ~730 RU; *black curves*) or DevAC (DevAC_i8H; ~510 RU; *gray curves*) to DevB ($DevB^{sol}$; *solid lines*) or $DevB^{N333A}$ ($DevB^{sol}$_N333A; *dashed lines*). DevB was injected in the reaction buffer at 2.0 μM. *D*, electron micrograph of a heterocyst of strain $DR74^{DevB}$. *HEP*, heterocyst envelope polysaccharide layer; *HGL*, glycolipid layer. *Error bar*, 1 μm. *E*, electron micrograph of a heterocyst of strain $DR74^{DevB\_N333A}$. *Bar*, 1 μm.

described as adaptors for different exporters specialized on their respective substrates (7, 8, 10). It can be assumed that TolC, the only OMF predicted from the *Anabaena* sp. PCC 7120 genome sequence (20), must complete further heterocyst development related (and unrelated) tasks after 9 h of nitrogen depletion. At least six close homologues of *devB* can be found in the *Anabaena* sp. PCC 7120 genome (*all0809*, *all2652*, *alr3647*, *alr4280*, *alr4973*, and *all5347*). They, and MFPs of other export systems, could also interact with TolC, and some of them had expression patterns similar to that of *devB* (data not shown). A mutant of *all5347* (*hgdB*) could not fix N_2 and showed aberrant HGL layers (29). To focus on TolC-DevBCA and to minimize the influence of other MFPs and the respective exporters, cross-linking studies were performed using filaments that had experienced 9 h of nitrogen deprivation because TolC seems to play a promiscuous role in cyanobacteria.

Glycolipid Export by an ATP-driven Efflux Pump—The correlation between the enrichment of HGLs (Fig. 3*B*) and the response of the ATPase activity of DevAC (Fig. 3*A*) clearly shows that HGLs are a substrate of DevBCA-TolC. Moieties of HGLs or proteins/other compounds, suspected to possibly be exported by DevBCA-TolC (20), could not be identified as substrates. Any impairment of TolC-DevBCA caused the accumulation of entire HGLs, but not of their moieties, in the cytoplasmic membrane fraction (Fig. 3*B*, *MT*, shown for the *devB* mutant $DR74^{DevB\_N333A}$). The moieties would have to be assembled after or during translocation to the cell surface (compare Lipid A (44, 45)). Other HGL components or intermediates have never been detected in *Anabaena* sp. PCC 7120 heterocysts in past studies (20, 29, 36, 46–49). Involvement of DevBCA-TolC in protein export was not observed; the response of DevAC did not differ for untreated and proteinase K-treated or boiled fractions. Nevertheless, the substrate specificity of DevBCA-TolC presented in this work must not necessarily reflect all substrates and functions *in vivo*. It is known that the homologous system MacAB-TolC, where MacA corresponds to DevB and MacB to DevAC, is involved in the export of macrolides but does not show any response in ATPase activity toward their presence, indicating that additional factors could be required for activity (38). Because DevBCA is tightly regulated at the stages of expression/degradation (Fig. 1*A*) and seems to export a specific substrate at a specific stage in hetero-

cyst differentiation, putative accessory factors may not be required for translocation/ATPase activity response.

Involvement of ABC exporters, *e.g.* the LolCDE- and MsbA systems, in lipoprotein/glycolipid export has been reported previously (50–54). The IMF DevAC does not show remarkable sequence similarities to MsbA but has higher homologies to the Gram-negative ABC exporter LolCDE, where LolCE corresponds to DevC and LolD to DevA. DevAC also shows high similarities to FtsEX (55, 56), where FtsX corresponds to DevC and FtsE to DevA. FtsEX is involved in cell division and is assumed to export salts. MsbA, LolCDE, and FtsEX are not known to interact with an OMF such as TolC. Taken together, no known ABC exporter involved in cell division/differentiation and in glycolipid transfer resembles the DevBCA-TolC export machinery of *Anabaena* sp. PCC 7120.

Prerequisites of Cyanobacterial Glycolipid Efflux Pump—Although *Anabaena* prefers a freshwater environment (pH 7.8 or higher), the optimal pH for TolC-DevB interaction appears to be 6.2 and is therefore similar to that required for MacA-TolC interaction in *E. coli* (pH 5.8 (Ref. 10)). The periplasm of Gram-negative bacteria is known to be more acidic than the cytoplasm and, in most cases, is more acidic than the surrounding medium (57). So far, there are no data showing a complete respiratory chain in the cytoplasmic membrane of any cyanobacteria. Consequently, there are no data on H^+ accumulation in the cyanobacterial periplasm (58). Cyanobacteria usually maintain a photosynthesis-driven H^+ gradient over the thylakoid membrane. Nevertheless, a heterocyst-specific acidification of the periplasm could be caused by increase in the respiratory rate in the cytoplasmic membrane of heterocysts to consume harmful oxygen (23) All0809, a close homologue of DevB, was localized in all cells of the filament and showed a binding optimum to TolC at higher pH.[3] Lower pH in the periplasm of heterocysts could favor the binding of DevB to TolC, simply because the complex is needed in this state of heterocyst development.

A "bridging model" was proposed for the TolC-DevBCA homologue TolC-MacAB, with a MacA hexamer fitting to the tip of TolC in a cogwheel-like manner (9, 40, 41). It was derived from *in silico* protein models based on MacA crystals resolved to hexamers and electron micrographs showing a barrel-like hexameric assembly. Furthermore, the IMF MacB was proposed to form dimers (37, 39) and the OMF TolC trimers (7, 8). Hence, a TolC:MacA:MacB ratio of 3:6:2 could be assumed. Our data on DevBCA-TolC support exactly this stoichiometry (Fig. 2). DevB_N333A does not seem to form stable hexamers (Fig. 3*C* and supplemental Fig. S3) and cannot make DevAC recognize the presence of HGLs *in vitro* (Fig. 3*A*). This mutant does not rescue the phenotype of a *devB* knock-out (Fig. 3*E*). These observations imply the importance of a hexameric bridge between IMF and OMF even *in vivo* (Fig. 3*E*). However, details on the connecting structures of DevB to TolC either bridging to or wrapping around the OMF (like that modeled for the resistance-nodulation-division exporter AcrAB (6, 8, 59)), cannot be predicted from our data. ABC exporters such as DevAC are anchored compactly into the cytoplasmic membrane and do not contact TolC directly (37–39). Therefore, a hexameric DevB tunnel separating the transport pathway from the periplasm could provide a distinct milieu for HGL export.

Evaluation of SPR and ITC data predicted two binding events of DevB to both TolC and DevAC (Fig. 2). Both affinities seem to be largely based on MFP behavior. Although the interaction of free DevB with immobilized TolC or DevAC is reproducible for a wide range of surface protein densities, the kinetics of the immobilized DevB with its ligands strongly depend on the concentration of DevB on the chip surface. The reaction parameters were comparable only when a high surface density of DevB was used. This could be due to the resulting enhanced possibility of surface-bound DevB forming one of the preferred states in solution, *i.e.* a hexamer (supplemental Fig. S3). The oligomerization pattern of DevB indicates that more binding events, including those involving the binding of MFP to MFP, could be expected. The reason for there being only two dominant (and therefore detectable) binding events could be a very stringent interaction behavior in the presence of OMF or IMF ligands and reflect either hexamer formation with subsequent ligand binding or an additional but yet unknown intermediate binding state.

In summary, our results suggest that TolC-DevBCA form an efflux pump required for the export of HGLs of the heterocyst cell wall in *Anabaena* sp. PCC 7120. DevB connects the IMF DevAC to the OMF TolC by forming a hexamer throughout the acidic periplasm. It can provide a separate lipophilic tunnel for the transport of lipophilic HGLs beyond the outer membrane. TolC-DevBCA can be considered as a uniquely adjusted system for the formation of an extracellular glycolipid layer in heterocysts. It is the first reported ATP-driven efflux pump that provides a novel pathway for glycolipid export.

Acknowledgments—We thank Claudia Menzel for preparing the electron microscopy samples and Oleksandra Fokina and Dr. Javier Espinosa for introduction into and support with SPR and ITC. Furthermore, we thank Professor Enrico Schleiff for critical discussion and helpful suggestions. We thank Professor C. Peter Wolk for pRL plasmids and Dr. A. Muro-Pastor for pCSEL24.

[3] P. Staron, K. Forchhammer, and I. Maldener, unpublished data.

REFERENCES

1. Piñero-Fernandez, S., Chimerel, C., Keyser, U. F., and Summers, D. K. (2011) *J. Bacteriol.* **193,** 1793–1798
2. Martins, M., Viveiros, M., Couto, I., Costa, S. S., Pacheco, T., Fanning, S., Pagès, J. M., and Amaral, L. (2011) *In Vivo* **25,** 171–178
3. Deininger, K. N., Horikawa, A., Kitko, R. D., Tatsumi, R., Rosner, J. L., Wachi, M., and Slonczewski, J. L. (2011) *PLoS ONE* **6,** e18960
4. Ferhat, M., Atlan, D., Vianney, A., Lazzaroni, J. C., Doublet, P., and Gilbert, C. (2009) *PLoS ONE* **4,** e7732
5. Hantke, K., Winkler, K., and Schultz, J. E. (2011) *J. Bacteriol.* **193,** 1086–1089
6. Symmons, M. F., Bokma, E., Koronakis, E., Hughes, C., and Koronakis, V. (2009) *Proc. Natl. Acad. Sci. U.S.A.* **106,** 7173–7178
7. Koronakis, V., Eswaran, J., and Hughes, C. (2004) *Annu. Rev. Biochem.* **73,** 467–489
8. Koronakis, V., Sharff, A., Koronakis, E., Luisi, B., and Hughes, C. (2000) *Nature* **405,** 914–919
9. Yum, S., Xu, Y., Piao, S., Sim, S. H., Kim, H. M., Jo, W. S., Kim, K. J., Kweon, H. S., Jeong, M. H., Jeon, H., Lee, K., and Ha, N. C. (2009) *J. Mol. Biol.* **387,** 1286–1297

10. Tikhonova, E. B., Dastidar, V., Rybenkov, V. V., and Zgurskaya, H. I. (2009) *Proc. Natl. Acad. Sci. U.S.A.* **106,** 16416–16421
11. Mikolosko, J., Bobyk, K., Zgurskaya, H. I., and Ghosh, P. (2006) *Structure* **14,** 577–587
12. Eswaran, J., Koronakis, E., Higgins, M. K., Hughes, C., and Koronakis, V. (2004) *Curr. Opin. Struct. Biol.* **14,** 741–747
13. Higgins, M. K., Bokma, E., Koronakis, E., Hughes, C., and Koronakis, V. (2004) *Proc. Natl. Acad. Sci. U.S.A.* **101,** 9994–9999
14. Lobedanz, S., Bokma, E., Symmons, M. F., Koronakis, E., Hughes, C., and Koronakis, V. (2007) *Proc. Natl. Acad. Sci. U.S.A.* **104,** 4612–4617
15. Holland, I. B., Schmitt, L., and Young, J. (2005) *Mol. Membr. Biol.* **22,** 29–39
16. Saier, M. H., Jr., Beatty, J. T., Goffeau, A., Harley, K. T., Heijne, W. H., Huang, S. C., Jack, D. L., Jähn, P. S., Lew, K., Liu, J., Pao, S. S., Paulsen, I. T., Tseng, T. T., and Virk, P. S. (1999) *J. Mol. Microbiol. Biotechnol.* **1,** 257–279
17. Tseng, T. T., Gratwick, K. S., Kollman, J., Park, D., Nies, D. H., Goffeau, A., and Saier, M. H., Jr. (1999) *J. Mol. Microbiol. Biotechnol.* **1,** 107–125
18. Fiedler, G., Arnold, M., and Maldener, I. (1998) *Biochim. Biophys. Acta* **1375,** 140–143
19. Fiedler, G., Arnold, M., Hannus, S., and Maldener, I. (1998) *Mol. Microbiol.* **27,** 1193–1202
20. Moslavac, S., Nicolaisen, K., Mirus, O., Al Dehni, F., Pernil, R., Flores, E., Maldener, I., and Schleiff, E. (2007) *J. Bacteriol.* **189,** 7887–7895
21. Maldener, I., Hannus, S., and Kammerer, M. (2003) *FEMS Microbiol. Lett.* **224,** 205–213
22. Kaneko, T., Nakamura, Y., Wolk, C. P., Kuritz, T., Sasamoto, S., Watanabe, A., Iriguchi, M., Ishikawa, A., Kawashima, K., Kimura, T., Kishida, Y., Kohara, M., Matsumoto, M., Matsuno, A., Muraki, A., Nakazaki, N., Shimpo, S., Sugimoto, M., Takazawa, M., Yamada, M., Yasuda, M., and Tabata, S. (2001) *DNA Res.* **8,** 205–213; 227–253
23. Wolk, C. P., Ernst, A., and Elhai, J. (1994) *The Molecular Biology of Cyanobacteria* (Bryant, D.A., ed.), pp. 769–823, Kluwer Academic, Dudrecht, The Netherlands
24. Fay, P. (1992) *Microbiol. Rev.* **56,** 340–373
25. Cardemil, L., and Wolk, C. P. (1976) *J. Biol. Chem.* **251,** 2967–2975
26. Haury, J. F., and Wolk, C. P. (1978) *J. Bacteriol.* **136,** 688–692
27. Gambacorta, A., Romano, I., Sodano, G., and Trincone, A. (1998) *Phytochemistry* **48,** 801–805
28. Campbell, E. L., Cohen, M. F., and Meeks, J. C. (1997) *Arch. Microbiol.* **167,** 251–258
29. Fan, Q., Huang, G., Lechno-Yossef, S., Wolk, C. P., Kaneko, T., and Tabata, S. (2005) *Mol. Microbiol.* **58,** 227–243
30. Awai, K., and Wolk, C. P. (2007) *FEMS Microbiol. Lett.* **266,** 98–102
31. Rippka, R., Dereules, J., Waterbury, J. B., Herdman, M., and Stanier, R. Y. (1979) *J. Gen. Microbiol.* **111,** 1–61
32. Wolk, C. P., Vonshak, A., Kehoe, P., and Elhai, J. (1984) *Proc. Natl. Acad. Sci. U.S.A.* **81,** 1561–1565
33. Olmedo-Verd, E., Muro-Pastor, A. M., Flores, E., and Herrero, A. (2006) *J. Bacteriol.* **188,** 6694–6699
34. Candiano, G., Bruschi, M., Musante, L., Santucci, L., Ghiggeri, G. M., Carnemolla, B., Orecchia, P., Zardi, L., and Righetti, P. G. (2004) *Electrophoresis* **25,** 1327–1333
35. Fokina, O., Chellamuthu, V. R., Zeth, K., and Forchhammer, K. (2010) *J. Mol. Biol.* **399,** 410–421
36. Winkenbach, F., Wolk, C. P., and Jost, M. (1972) *Planta* **107,** 69–80
37. Lin, H. T., Bavro, V. N., Barrera, N. P., Frankish, H. M., Velamakanni, S., van Veen, H. W., Robinson, C. V., Borges-Walmsley, M. I., and Walmsley, A. R. (2009) *J. Biol. Chem.* **284,** 1145–1154
38. Tikhonova, E. B., Devroy, V. K., Lau, S. Y., and Zgurskaya, H. I. (2007) *Mol. Microbiol.* **63,** 895–910
39. Xu, Y., Sim, S. H., Nam, K. H., Jin, X. L., Kim, H. M., Hwang, K. Y., Lee, K., and Ha, N. C. (2009) *Biochemistry* **48,** 5218–5225
40. Xu, Y., Song, S., Moeller, A., Kim, N., Piao, S., Sim, S. H., Kang, M., Yu, W., Cho, H. S., Chang, I., Lee, K., and Ha, N. C. (2011) *J. Biol. Chem.* **286,** 13541–13549
41. Xu, Y., Sim, S. H., Song, S., Piao, S., Kim, H. M., Jin, X. L., Lee, K., and Ha, N. C. (2010) *Biochem. Biophys. Res. Commun.* **394,** 962–965
42. Kim, H. M., Xu, Y., Lee, M., Piao, S., Sim, S. H., Ha, N. C., and Lee, K. (2010) *J. Bacteriol.* **192,** 4498–4503
43. Nicolaisen, K., Hahn, A., and Schleiff, E. (2009) *J. Basic Microbiol.* **49,** 5–24
44. Raetz, C. R., Ulevitch, R. J., Wright, S. D., Sibley, C. H., Ding, A., and Nathan, C. F. (1991) *FASEB J.* **5,** 2652–2660
45. Raetz, C. R., Reynolds, C. M., Trent, M. S., and Bishop, R. E. (2007) *Annu. Rev. Biochem.* **76,** 295–329
46. Black, K., Buikema, W. J., and Haselkorn, R. (1995) *J. Bacteriol.* **177,** 6440–6448
47. Ramírez, M. E., Hebbar, P. B., Zhou, R., Wolk, C. P., and Curtis, S. E. (2005) *J. Bacteriol.* **187,** 2326–2331
48. Shi, L., Li, J. H., Cheng, Y., Wang, L., Chen, W. L., and Zhang, C. C. (2007) *J. Bacteriol.* **189,** 5075–5081
49. Bauersachs, T., Compaoré, J., Hopmans, E. C., Stal, L. J., Schouten, S., and Sinninghe Damsté, J. S. (2009) *Phytochemistry* **70,** 2034–2039
50. Narita, S., and Tokuda, H. (2006) *FEBS Lett.* **580,** 1164–1170
51. Narita, S., and Tokuda, H. (2010) *Methods Mol. Biol.* **619,** 117–129
52. Siarheyeva, A., and Sharom, F. J. (2009) *Biochem. J.* **419,** 317–328
53. Kaul, G., and Pattan, G. (2011) *Indian J. Biochem. Biophys.* **48,** 7–13
54. Eckford, P. D., and Sharom, F. J. (2010) *Biochem. J.* **429,** 195–203
55. Garti-Levi, S., Hazan, R., Kain, J., Fujita, M., and Ben-Yehuda, S. (2008) *Mol. Microbiol.* **69,** 1018–1028
56. Schmidt, K. L., Peterson, N. D., Kustusch, R. J., Wissel, M. C., Graham, B., Phillips, G. J., and Weiss, D. S. (2004) *J. Bacteriol.* **186,** 785–793
57. Wilks, J. C., and Slonczewski, J. L. (2007) *J. Bacteriol.* **189,** 5601–5607
58. Schultze, M., Forberich, B., Rexroth, S., Dyczmons, N. G., Roegner, M., and Appel, J. (2009) *Biochim. Biophys. Acta* **1787,** 1479–1485
59. Touzé, T., Eswaran, J., Bokma, E., Koronakis, E., Hughes, C., and Koronakis, V. (2004) *Mol. Microbiol.* **53,** 697–706